# Quantification of ocular surface microcirculation by computer assisted video microscopy and diffuse reflectance spectroscopy

Anne Kari Kvernebo [a,b,c,*], Takuma Miyamoto [d], Ane Hasle Sporastøyl [c,e],
Liv Kristin Wikslund [c,e], Svein-Erik Måsøy [f], Liv Drolsum [a,b], Morten Carstens Moe [a,b],
Goran Salerud [g], Kiyotaka Fukamachi [d], Knut Kvernebo [b,c]

[a] Department of Ophthalmology, Oslo University Hospital HF, Postboks 4950 Nydalen, 0424, Oslo, Norway
[b] Institute of Clinical Medicine, Faculty of Medicine, University of Oslo, P.O. Box 1171 Blindern, 0318, Oslo, Norway
[c] The Circulation Laboratory, Department of Cardiothoracic Surgery, Oslo University Hospital HF, Postboks 4950 Nydalen, 0424, Oslo, Norway
[d] Lerner Research Institute, Department of Biomedical Engineering, 9500 Euclid Ave, ND20, Cleveland, OH, 44195, USA
[e] The Medical Student Research Program, Faculty of Medicine, University of Oslo, P.O. Box 1078 Blindern, 0318, Oslo, Norway
[f] ODI Medical AS, Gaustadalléen 21, 0349, Oslo, Norway
[g] Department of Biomedical Engineering, Linkoping University, Campus US, SE-581 83, Linkoping, Sweden

## A R T I C L E   I N F O

## A B S T R A C T

In piglets we tested the applicability of digital video microscopy and diffuse reflectance spectroscopy for non-invasive assessments of limbal and bulbar conjunctival microcirculation. *A priori* we postulated that the metabolic rate is higher in limbal as compared to bulbar conjunctiva, and that this difference is reflected in microvascular structure or function between the two locations. Two study sites, Oslo University Hospital (OUH), Norway and Cleveland Clinic (CC), USA, used the same video microscopy and spectroscopy techniques to record limbal and bulbar microcirculation in sleeping piglets. Recordings were analyzed with custom-made software to quantify functional capillary density, capillary flow velocity and microvascular oxygen saturation in measuring volumes of approximately 0.1 mm$^3$. The functional capillary density was higher in limbus than in bulbar conjunctiva at both study sites (OUH: $18.1 \pm 2.9$ versus $12.2 \pm 2.9$ crossings per mm line, $p < 0.01$; CC: $11.3 \pm 3.0$ versus $7.1 \pm 2.8$ crossings per mm line, $p < 0.01$). Median categorial capillary blood flow velocity was higher in bulbar as compared with limbal recordings (CC: 3 (1–3) versus 1 (0–3), $p < 0.01$). Conjunctival microvascular oxygen saturation was $88 \pm 5.9\%$ in OUH versus $94 \pm 7.5\%$ in CC piglets.

Non-invasive digital video microscopy and diffuse reflectance spectroscopy can be used to obtain data from conjunctival microcirculation in piglets. Limbal conjunctival microcirculation has a larger capacity for oxygen delivery as compared with bulbar conjunctiva.

## 1. Introduction

August Krogh, the Nobel prize laureate in Physiology or Medicine in 1920, postulated that metabolically active cells must be located within a given distance of a perfused capillary (the Krogh diameter) to get sufficient oxygen supply (Krogh, 1919). He stated that within the tissue cylinder served by one capillary, the oxygen availability decreases exponentially at increasing distances from the center of the vessel. Cells outside such a cylinder will suffer from hypoxia, independent of the blood flow in the capillary.

The main functions of conjunctival vessels are to transport and deliver oxygen and nutrients for metabolic needs, serve thermoregulation of the eye and serve a "watch out" function in case of infection or inflammation. In the limbal region, self-renewing epithelial stem cells are more numerous than other areas of conjunctiva (Ramos et al., 2015). Studies imply that limbal stem cells are crucial for maintaining the physiological border between the conjunctiva and the avascular cornea (Notara et al., 2018), and also provide corneal epithelial homeostasis. In a healthy bulbar conjunctiva, the metabolic demand can be postulated

**Abbreviations**

| | |
|---|---|
| CC | Cleveland Clinic |
| CFV | capillary flow velocity |
| FCD | functional capillary density |
| ODIN | Oxygen delivery index |
| OUH | Oslo University Hospital |
| $SmvO_2$ | microvascular oxygen saturation |

to be lower than the limbal region as the main function is to sustain an intact translucent epithelial surface and supply nutrition to the underlying sclera.

Several techniques have been used for measurements of different aspects of conjunctival microcirculation, like conjunctival vessel density and blood flow velocities. In addition, sensors have been used for measuring oxygen tension (Fenton et al., 1979; Iguchi et al., 2005; Kwan and Fatt, 1971; Li et al., 2015; Shi et al., 2019; Shoemaker and Lawner, 1983; van Zijderveld et al., 2014; Xu et al., 2015). These technologies have, however, not been used for estimating the oxygen delivery from the capillaries to the cells, which is the most important function of the circulatory system.

Oxygen Delivery INdex (ODIN) is a non-invasive concept, for assessment of oxygen delivery from the microcirculation to tissue cells in measuring volumes of approximately 0.1 mm$^3$. *In vivo* digital microscopy and spectroscopy, mounted in a mobile microvascular laboratory (mLab), are used for data file acquisition. Three parameters; Functional capillary density (FCD), capillary flow velocities (CFV) and microvascular oxygen saturation ($SmvO_2$) are quantified during analysis. Results provide reproducible values for skin measurements (Fredly et al., 2015) and have a high sensitivity for detecting reduced oxygen delivery during systemic circulatory failure in both animal models and in healthy and sick humans (Awan et al., 2011; Fredly et al., 2016; Wester et al., 2011, 2014).

In piglets, our main aim was to test applicability of the ODIN concept for conjunctival microvascular measurements. As cell division and accordingly the metabolic rate and oxygen demand can be postulated to be higher at the limbus as compared to the bulbar conjunctiva, we also aimed to examine and validate sensitivity of the ODIN concept by comparing microvascular physiology in limbal and bulbar conjunctiva.

## 2. Material and methods

### 2.1. Study population

Experiments were performed in two laboratories with common research interests: Oslo University Hospital (OUH), Norway and Cleveland Clinic (CC), USA. The conjunctival microcirculation of five Norwegian landrace piglets of both sexes (30 ± 3 kg) (OUH) and eight female Yorkshire piglets (44 ± 4 kg) (CC) was recorded. The study at OUH was approved by the Norwegian Food Safety Authority (FOTS, id: 6689). At CC, the study protocols were approved by Institutional Animal Care and Use Committee (study number 2016-1659). The animals received humane care in compliance with the Guide for the Care and Use of Laboratory Animals and institutional guidelines.

### 2.2. Equipment for microvascular examinations

Both study sites used a mobile microvascular laboratory (mLab, version α1, ODI Medical AS, Oslo, Norway), containing a digital video microscope, a spectroscope and a computer with custom made software.

#### 2.2.1. Digital microscopy

A digital hand-held video-microscope (Optilia, D1, Instruments AB, Sollentuna, Sweden) with a 300 × magnification lens, image resolution of 1920 × 1080 pixels, field of view of 1.13 mm × 0.7 mm and frame rate of seven frames per second was used to obtain conjunctival recordings of 20 seconds duration.

One operator (AKK) conducted analyses off-line using a custom-made software (EyeSoft version 1.0, ODI). Adjustments of light intensity, contrast and tint optimized the image quality. In limbal recordings, a line touching the edge of the cornea was created by the operator. An additional five parallel lines separated by 100 μm were created by the software at increasing distances from the cornea (Fig. 1a). In films from the bulbar conjunctiva, six horizontal lines separated by 100 μm were drawn (Fig. 1b).

Capillaries (blood vessels < 20 μm) containing erythrocytes crossing the lines were identified and marked manually. Empty capillaries are not seen by the microscope. FCD was expressed as capillary crossings/mm line (c/mm).

In the CC series, CFV at each capillary crossing was determined according to a six-category velocity scale (Table 1). If the velocity fluctuated during a film sequence, the average velocity throughout the film was used. Data were expressed as the fraction of capillaries in each blood flow category. Malfunctioning software compressed recorded OUH films upon storage, and velocity profiles could not be assessed.

#### 2.2.2. Spectroscopy

The Diffuse Reflectance Spectroscopy (DRS) system used in this study has a measuring volume in the range of 0.1 mm$^3$ (Sundheim et al., 2017). A halogen light source (AvaLight-HAL, Avantes, Apeldoorn, The Netherlands) with spectral range 450–800 nm, and a measuring probe (FCR-7uv400-2.3-bx, Avantes) with six emitting and one receiving 400 μm fibers were connected to a spectrometer (AvaSpec-2048-2, Avantes). Calibration was performed before and after each set of measurements by holding the probe against a white polytetrafluorethylene tile (WS-2, Avantes).

The DRS spectra analyses were carried out with the help of a simplified tissue model, that calculates light propagation in the tissue, using the approach from Farrell (Farrell et al., 1992) and Jacques (2013). Starting with a set of initial propagation parameters for the tissue, the model implemented in Python/MATLAB, produced a spectrum that is compared to the acquired DRS to calculate the optimal propagation parameters that reproduce the best fit to the data. Finally, the oxyhemoglobin and deoxyhemoglobin concentrations were calculated.

#### 2.2.3. Pulse oximetry

The arterial oxygen saturation was monitored by a pulse oximeter attached to the tail (OUH: Capnostream 20p, Oridion Medical, Israel) or the ear (CC: Aisys CS2, GE healthcare, Illinoi U.S.).

### 2.3. Laboratory procedure

Different definitions of "limbus" exist (Van Buskirk, 1989). In the present study, the limbus is referred to as the surface of the eye where the transparent corneal and the opaque vascularized conjunctival tissue fuse (Fig. 2). The bulbar conjunctiva was defined as the conjunctival tissue located at least 2 mm away from the limbus.

At both study sites, conjunctival microvascular baseline data were collected from the left eye following general anesthesia and prior to other planned experiments.

At OUH, the piglets acclimatized in a cubicle with free access to water and food three to six days prior to the study. The piglets were sedated by injecting narketan/ketamine (11/33 mg/kg) intramuscularly in the neck. Fentanyl (30–100 μg/kg/h) and propofol (12–20 mg/kg/h) injections induced general anesthesia. The piglets were fixed in a supine position and orotracheally intubated. When stable in general anesthesia, a tracheostomy was performed, and an endotracheal tube inserted. Venous access for infusions and blood samples were secured by a
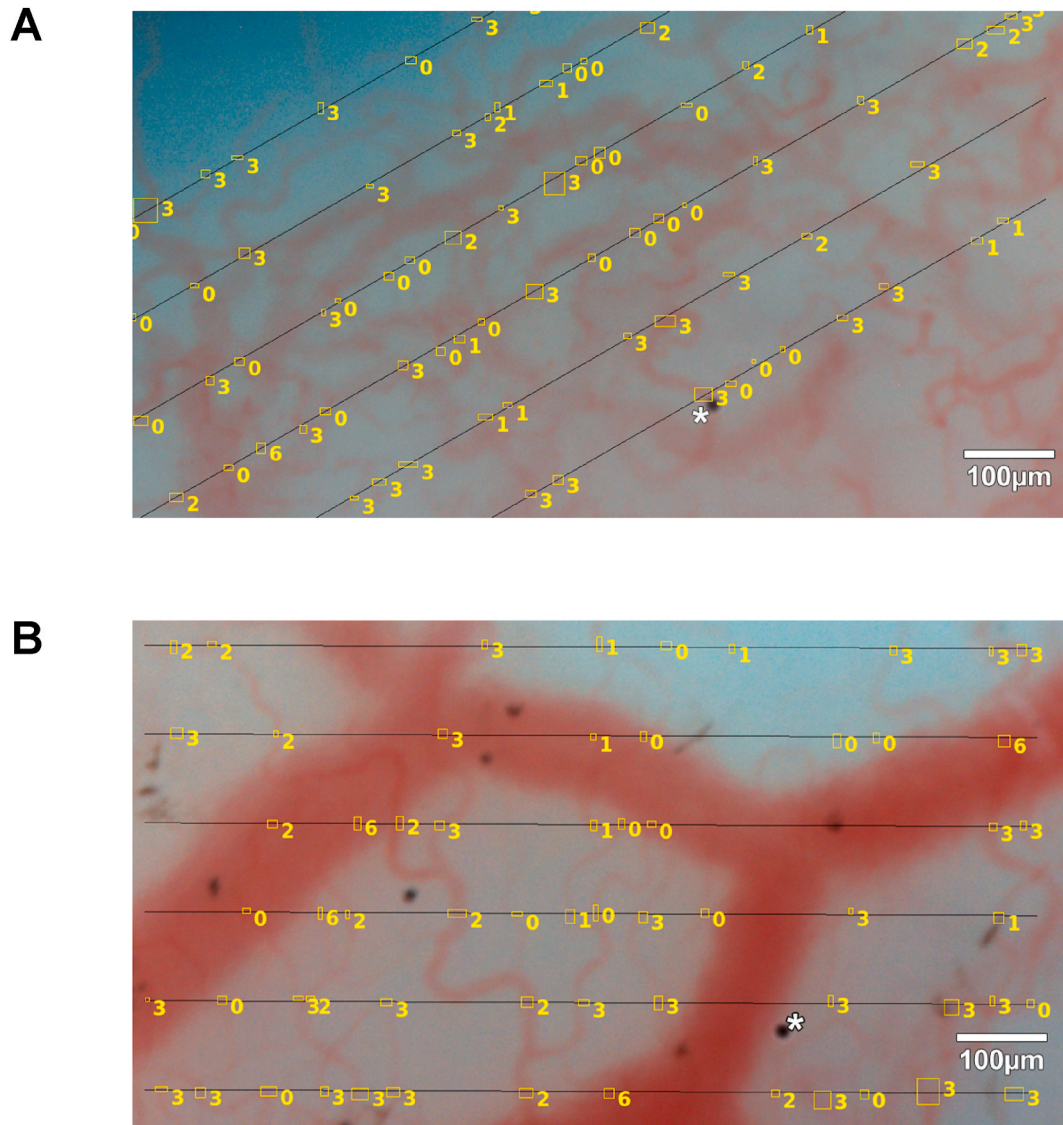
**Fig. 1.** Photo taken during analysis. Yellow boxes identify capillaries crossing six parallel lines. The number besides each box represents capillary flow velocity category. Vessels larger than 20 μm are not included in the analyses. Black dots (*) seen in both frames are melanin aggregates. **A:** Frame from limbus. Avascular cornea seen in the upper left corner. **B:** Frame from bulbar conjunctiva. (For interpretation of the references to colour in this figure legend, the reader is referred to the Web version of this article.)

**Table 1**
Categories of capillary flow velocities.

| Blood flow category | Description of blood flow |
| --- | --- |
| 0 | No flow: Visible erythrocytes, no movement |
| 1 | Sluggish flow: Intermittent slow flow |
| 2 | Slow flow: Continuous slow flow or Intermittent "no flow" and rapid flow |
| 3 | Continuous flow |
| 4 | Rapid flow: Continuous rapid flow or Intermittent slow and brisk flow |
| 5 | Brisk flow: Continuous brisk flow |
| 6 | Uncertain: Velocity impossible to determinate |

catheter in the jugular vein. A catheter in the common carotid artery was used for monitoring blood pressure and sampling for blood gas analyses. A surgically inserted catheter in the urinary bladder measured urinary output and body temperature. Following surgery, the animals were placed on the right side before data acquisition. Finishing all experiments, the animals were euthanized by IV injection of potassium

chloride.

At CC, the animals were quarantined and monitored for at least three days prior to the study. Each piglet fasted for 12 h prior to surgery. As pre-medication, xylazine (2 mg/kg, IM) and ketamine (20 mg/kg, IM) were administered. Propofol (1 mg/kg, IV) or buprenorphine (0.05 mg/kg, IV) induced general anesthesia. The piglets had an endotracheal tube installed, and anesthesia was maintained by isoflurane gas (1.0–3.0%). The temperature was monitored by a rectal thermometer (Aisys CS2 GE healthcare, Illinoi, U.S.). The animal was placed in a supine position, and then given lidocaine (up to 2 mg/kg/h IV) to prevent ventricular arrhythmia. At the end of the studies, the animal was heparinized (500 U/mg) and sacrificed by administration of potassium chloride (2.5–3.5 mEq/kg, IV) under deep anesthesia with isoflurane (5%).

*2.4. Conjunctival microvascular measurements*

The same protocol was used for data acquisition at the two study sites. Microscopy films were recorded from two locations: The limbus (<1 mm from the cornea, i.e. cornea seen in part of the frames) and the bulbar conjunctiva (>2 mm away from the cornea). Isotone saline was
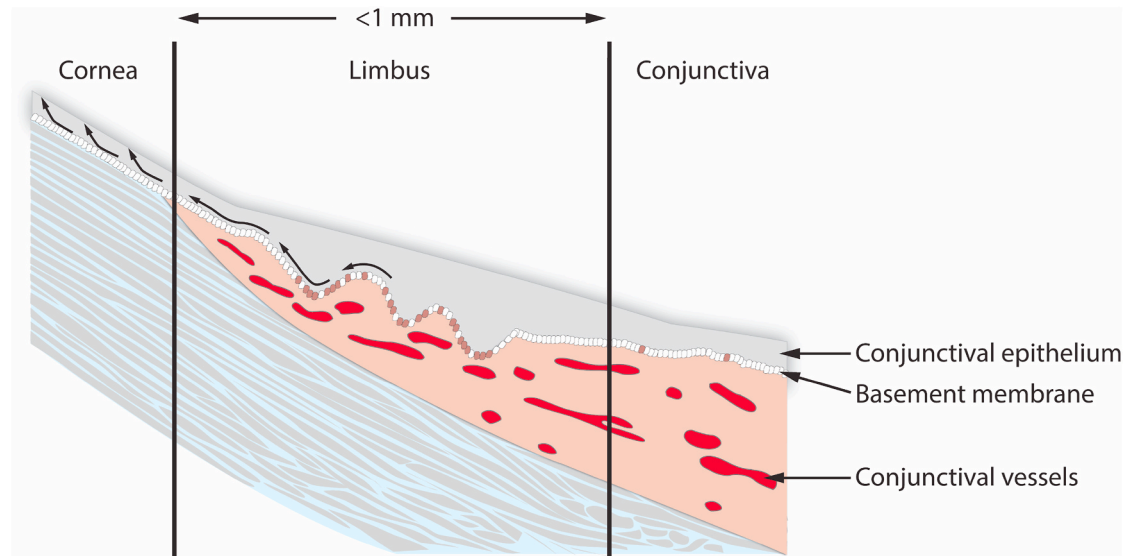
**Fig. 2.** Anatomy at the limbus and the bulbar conjunctiva. Brown dots represent stem cells embedded in the basement membrane. (For interpretation of the references to colour in this figure legend, the reader is referred to the Web version of this article.)

applied to the eye prior to recordings. At least four film sequences were recorded from both locations. DRS spectra were collected from the conjunctiva, but we did not reach sufficient precision of the probe position to differentiate between limbal and bulbar recordings.

### 2.5. Statistics

Functional capillary density and $SmvO_2$ results are presented as mean $\pm$ standard deviation and displayed as box-whisker plots. Comparing FCD from the limbus and the bulbar conjunctiva, an independent samples *t*-test, with a significance level of 5% was used. CFV data are presented as median with interquartile range and displayed in a histogram. Mann Whitney *U* test was applied to compare CFV data from limbus and bulbus. The statistical analysis was performed by SPSS version 25 (SPSS Inc, Chicago, Illinois, USA).

### 3. Results

It was possible to obtain microscopy films and DRS spectra from all piglets both at OUH and CC. No adverse events were recorded during data collection.

### 3.1. Functional capillary density (FCD)

We recorded 119 films, of which 47 were of inferior image quality and excluded from analyses. We analyzed 3422 capillaries (Table 2). At both study sites, the FCD was higher at limbus as compared with the bulbar conjunctiva (OUH: $18.1 \pm 2.9$ versus $12.2 \pm 2.9$ c/mm, p < 0.01, CC: $11.3 \pm 3.0$ versus $7.1 \pm 2.8$ c/mm, p < 0.01) (Fig. 3).

**Table 2**
Number of microscopy films and analyzed capillaries. Capillary blood flow velocity is only scored in data from Cleveland Clinic and not in the Oslo University Hospital series due to quality of the films.

|  |  | OUH | CC |
|---|---|---|---|
| Total number of recorded films |  | 49 | 70 |
| Number of analyzed films | Limbus | 19 | 24 |
|  | Bulbar conjunctiva | 17 | 12 |
| Number of analyzed capillaries | Limbus | 1533 | 526 |
|  | Bulbar conjunctiva | 1135 | 228 |

### 3.2. Capillary flow velocity (CFV)

The most prominent flow categories were 0 (no flow) in limbus and 3 (continuous flow) in bulbar conjunctiva (Fig. 4). Median categorial CFV was higher in bulbar recordings as compared with limbal recordings (CC: 3 (1–3) versus 1 (0–3), p < 0.01).

### 3.3. Microvascular oxygen saturation (SmvO2)

All piglets at both study sites had pulse-oximetry assessed arterial oxygen saturation $\geq 95\%$. Twenty-nine DRS spectra from Oslo and 91 from Cleveland were analyzed (Fig. 5). The remaining spectra were excluded due to heavy conjunctival melanosis or that the DRS algorithm failed to calculate saturation values in recordings with tissue hematocrit values below 0.01%. Mean microvascular oxygen saturation was high at both study sites (OUH: $88 \pm 5.9\%$, CC: $94 \pm 7.5\%$).

### 4. Discussion

The present study indicates that non-invasive digital video microscopy and diffuse reflectance spectroscopy can be used to obtain data from conjunctival microcirculation. In a piglet model, two independent sites found that limbal conjunctival microcirculation had a larger capacity for oxygen delivery as compared with bulbar conjunctiva measured by the ODIN concept.

August Krogh recognized that limited diffusion capacity of oxygen in vertebrate tissues has been the main determinant for the evolution of microvascular morphology and physiology. One hundred years later, technologies measuring microvascular oxygen delivery in routine clinical medicine is still absent. Conjunctival vessels have previously been studied by microscopy and oxygen tensions have been estimated by different sensors. This study was designed to test the conjunctival applicability of the ODIN concept in two similar settings, using *in vivo* microscopy and spectroscopy for assessing oxygen delivery.

The ODIN concept includes standardized technologies, a data acquisition protocol and analyses quantifying FCD, CFV and $SmvO_2$. This is a new diagnostic tool, that has been applied both in animal and human studies. Published and ongoing research has focused on papillary capillary circulation of the skin in healthy and severely sick neonates, patients with acute and chronic heart failure and early warning of systemic inflammatory syndrome in acute pancreatitis, sepsis and covid-19 infected (Awan et al., 2011; Fredly et al., 2015, 2016; Sundheim et al.,
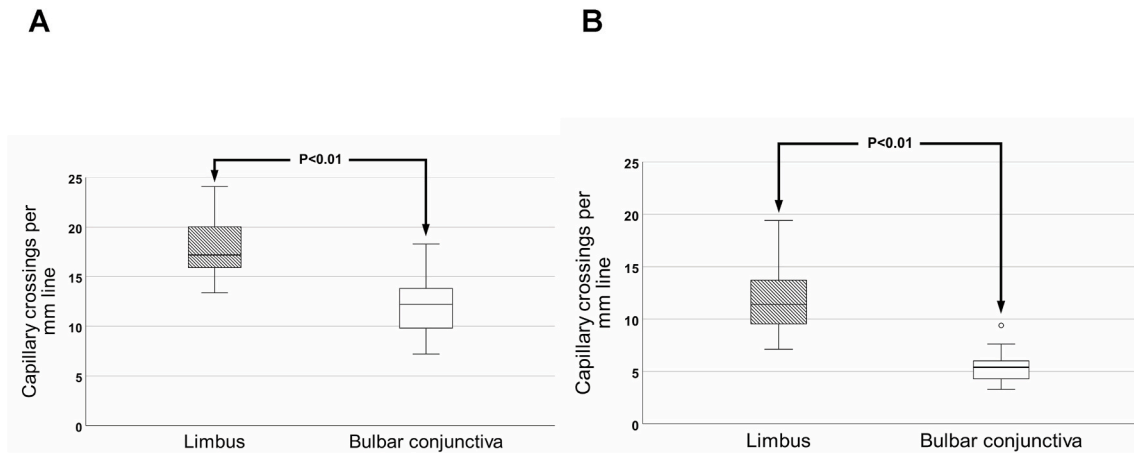
A

B



**Fig. 3.** Functional capillary density at limbus and bulbar conjunctiva in Oslo University Hospital (A) and Cleveland Clinic (B).
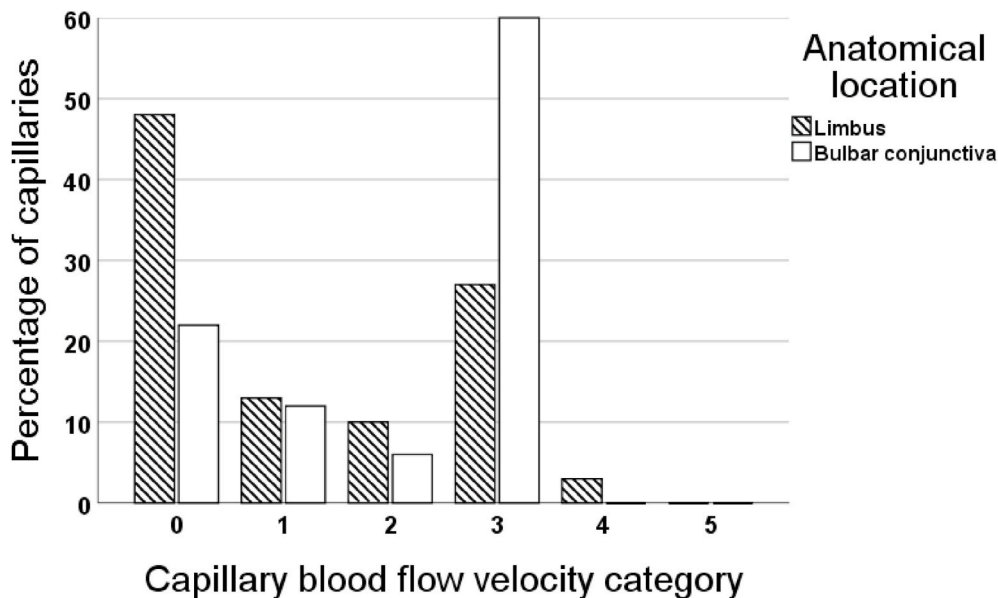


**Fig. 4.** Capillary flow velocity distribution at the limbus and bulbar conjunctiva (Cleveland Clinic recordings).

2017; Wester et al., 2011, 2014).

The conjunctiva adds a new window of examination in patients with systemic or local eye circulatory failure (e.g. glaucoma, diabetes and ischemia). In ophthalmology, one could potentially use the ODIN concept to quantify ocular surface injuries, in guiding treatment options and predict healing potential. Given that the retina and bulbar conjunctiva share the same embryological ectodermal origin (Swamynathan, 2013) and vascular supply, the microcirculation of the conjunctiva may also mirror the microcirculation of the central nervous system in patients with both systemic circulatory failure and brain pathology (e.g. ischemic stroke or high intracranial pressure).

Main determinants for oxygen delivery are capillary density, capillary blood flow velocities and oxygen saturation. Studies of cancer cell growth have shown that the maximal oxygen diffusion distance from a perfused vessel before chronic hypoxia develops ranges between 40 and 140 μm (Forster et al., 2017). Cell necrosis is seen at distances from 80 to 300 μm from a perfused vessel. In this study there was higher FCD in limbal recordings as compared with bulbar recordings. The bulbar FCD in the OUH piglets of 12.2 ± 2.9 c/mm was comparable to reported findings in the groin skin of piglets of the same breed 10.4 and 13.2 c/mm (Awan et al., 2011). The FCD results reported in this study are also within the same range as results from skin of the hand (12.4 ± 1.6

c/mm) and chest (10.7 ± 1.6 c/mm) of newborns (Fredly et al., 2015). The similar FCD results among different species and different tissues indicate that the oxygen diffusion capacity in vertebrae tissue is a common denominator for the evolutional development of microvascular densities. Furthermore, the differences in limbal and bulbar densities indicate higher metabolic activity in limbus.

Capillaries specialize in gas-equilibration, while larger vessels having a thicker diffusion barrier is of minor importance for oxygen delivery to cells (Akons et al., 2017). Still some degree of oxygen delivery will take place from arterioles. Since this factor is of minor importance for oxygen delivery in the current setting, we have excluded arterioles from the data presentation. If we had included the arterioles, the differences between bulbar and limbal densities would have been less, but still be present.

In capillaries, low blood flow velocities (category 0 and 1) prolong the erythrocyte's transit time, facilitating oxygen delivery. High blood flow velocities (categories 4 and 5) transform capillaries into physiological shunt vessels with insufficient transit time for oxygen equilibration. Continuous flow (category 3) is seen in more than 70% of capillaries in healthy human skin (Fredly et al., 2015; Sundheim et al., 2017; Wester et al., 2014). Presumably, category 3 flow is the optimal physiological velocity with respect to the number of erythrocytes
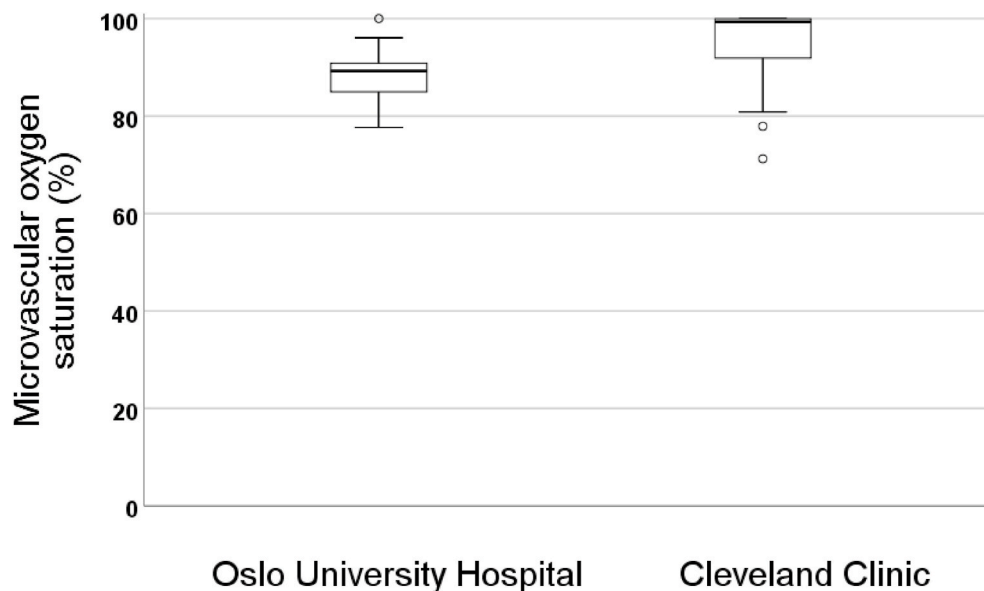
**Fig. 5.** Conjunctival microvascular oxygen saturation from Oslo University Hospital and Cleveland Clinic.

passing through a capillary and available time for oxygen delivery. In our study, median categorical CFV was higher in bulbar conjunctiva than limbus (CC: 3 (1–3) versus 1 (0–3)), and in both locations fewer capillaries had velocity category 3 flow as compared with previous reports from healthy human skin. The large spread in velocities in the present study is also seen in other piglet studies, and may be caused by anesthesia and supine positioning during measurements (Wester et al., 2011). The lower velocities in limbus give longer transit time for the erythrocytes and more time for oxygen delivery.

The spectroscope probe in this study covers approximately the same area as the microscopy frames: $\approx 1$ mm$^2$. In comparison, the limbus has a width of less than 1 mm. The DRS equipment used in this study did not allow for sufficient precision of probe positioning to differentiate between limbal and bulbar DRS recordings, and DRS data can accordingly not be compared between limbus and bulbar conjunctiva. The conjunctival SmvO$_2$ values (OUH: $88 \pm 5.9\%$ and CC: $94 \pm 7.5\%$) were higher in the CC than OUH piglets, but this difference may be due to lack of precision in probe positions during recordings. The SmvO$_2$ values were also considerably higher than what is reported from skin of piglets and humans (Awan et al., 2011; Fredly et al., 2015; Sundheim et al., 2017), indicating a high physiological reserve capacity of oxygen delivery. Since the partial pressure of oxygen in air is higher than in the lung alveoli ($\approx 160$ mm Hg versus 104 mm Hg), it is also possible that oxygen diffuses directly from the air into conjunctival capillary erythrocytes.

There are some study limitations. The microscopes film sampling frequency of 7 frames/s, reduces the precision of velocity assessments. Secondly, due to software problems, velocity profiles could not be determined in OUH films. In addition, the positioning of the DRS probe was too inaccurate to distinguish between the anatomical locations of the recorded spectra. For future studies, technological improvements and trained personnel for data acquisition can contribute to optimized image quality and precision during recordings. Software that is currently in development, will detect capillary density and velocity scores automatically in the future. Finally, comparative studies of the current technology compared to novel anterior optical coherence tomography angiography (OCTA) of ocular surface microcirculation are needed.

## 5. Conclusions

This study shows that the microscopy and spectroscopy techniques can safely be applied to the conjunctiva and have sufficient resolution

for analyses of the three ODIN variables essential for oxygen delivery. Differences between the two conjunctival regions were found at both study sites, supporting that the ODIN concept is able to detect a higher metabolic rate in limbus as compared to bulbus. With further refinement, this technology may be a supplement to standardized ocular examinations in humans, offering detailed understanding of microvascular pathology in patients with local eye circulatory conditions and/or systemic circulatory failure.

with images and graphical figures.

## References

Akons, K., Dann, E.J., Yelin, D., 2017. Measuring blood oxygen saturation along a capillary vessel in human. Biomed. Optic Express 8, 5342–5348.

Awan, Z.A., Häggblad, E., Wester, T., Kvernebo, M.S., Halvorsen, P.S., Kvernebo, K., 2011. Diffuse reflectance spectroscopy: systemic and microvascular oxygen saturation is linearly correlated and hypoxia leads to increased spatial heterogeneity of microvascular saturation. Microvasc. Res. 81, 245–251.

Farrell, T.J., Patterson, M.S., Wilson, B., 1992. A diffusion theory model of spatially resolved, steady-state diffuse reflectance for the noninvasive determination of tissue optical properties in vivo. Med. Phys. 19, 879–888.

Fenton, B.M., Zweifach, B.W., Worthen, D.M., 1979. Quantitative morphometry of conjunctival microcirculation in diabetes mellitus. Microvasc. Res. 18, 153–166.

Forster, J.C., Harriss-Phillips, W.M., Douglass, M.J., Bezak, E., 2017. A review of the development of tumor vasculature and its effects on the tumor microenvironment. Hypoxia 5, 21–32.

Fredly, S., Fugelseth, D., Nygaard, C.S., Salerud, E.G., Stiris, T., Kvernebo, K., 2016. Noninvasive assessments of oxygen delivery from the microcirculation to skin in hypothermia-treated asphyxiated newborn infants. Pediatr. Res. 79, 902–906.

Fredly, S., Fugelseth, D., Wester, T., Häggblad, E., Kvernebo, K., 2015. Skin microcirculation in healthy term newborn infants–assessment of morphology, perfusion and oxygenation. Clin. Hemorheol. Microcirc. 59, 309–322.

Iguchi, S., Mitsubayashi, K., Uehara, T., Ogawa, M.J.S., Chemical, A.B., 2005. A Wearable Oxygen Sensor for Transcutaneous Blood Gas Monitoring at the Conjunctiva, vol. 108, pp. 733–737.

Jacques, S.L., 2013. Optical properties of biological tissues: a review. Phys. Med. Biol. 58, R37–R61.

Krogh, A., 1919. The supply of oxygen to the tissues and the regulation of the capillary circulation. J. Physiol. 52, 457–474.

Kwan, M., Fatt, I., 1971. A noninvasive method of continuous arterial oxygen tension estimation from measured palpebral conjunctival oxygen tension. Anesthesiology 35, 309–314.

Li, Y., Lu, C.D., Jia, Y., Lee, B., Kraus, M.F., Hornegger, J., Fujimoto, J.G., Huang, D., 2015. Anterior segment angiography with 1050 nm swept-source optical coherence tomography. Invest. Ophthalmol. Vis. Sci. 56, 4512-4512.

Notara, M., Lentzsch, A., Coroneo, M., Cursiefen, C., 2018. The role of limbal epithelial stem cells in regulating corneal (Lymph)angiogenic privilege and the micromilieu of the limbal niche following UV exposure. Stem Cell. Int. 8620172, 2018.

Ramos, T., Scott, D., Ahmad, S., 2015. An update on ocular surface epithelial stem cells: cornea and conjunctiva. Stem Cell. Int. 2015, 601731.

Shi, C., Jiang, H., Gameiro, G.R., Wang, J., 2019. Microcirculation in the conjunctiva and retina in healthy subjects. Eye and vision (London, England) 6, 11.

Shoemaker, W.C., Lawner, P.M., 1983. Method for continuous conjunctival oxygen monitoring during carotid artery surgery. Crit. Care Med. 11, 946–947.

Sundheim, L.K., Sporastøyl, A.H., Wester, T., Salerud, G., Kvernebo, K., 2017. Acute Skin Trauma Induces Hyperemia, but Superficial Papillary Nutritive Perfusion Remains Unchanged. Microcirculation, New York, N.Y., p. 24, 1994.

Swamynathan, S.K., 2013. Ocular surface development and gene expression. Journal of Ophthalmology 2013, 103947.

Van Buskirk, E.M., 1989. The anatomy of the limbus. Eye 3, 101–108.

van Zijderveld, R., Ince, C., Schlingemann, R.O., 2014. Orthogonal polarization spectral imaging of conjunctival microcirculation. Graefe's archive for clinical and experimental ophthalmology = Albrecht von Graefes Archiv fur klinische und experimentelle Ophthalmologie 252, 773–779.

Wester, T., Awan, Z.A., Kvernebo, T.S., Salerud, G., Kvernebo, K., 2014. Skin microvascular morphology and hemodynamics during treatment with veno-arterial extra-corporeal membrane oxygenation. Clin. Hemorheol. Microcirc. 56, 119–131.

Wester, T., Häggblad, E., Awan, Z., Barratt-Due, A., Kvernebo, M., Halvorsen, P., Mollnes, T., Kvernebo, K.J.C.p., imaging, f., 2011. Assessments of Skin and Tongue Microcirculation Reveals Major Changes in Porcine Sepsis, vol. 31, pp. 151–158.

Xu, Z., Jiang, H., Tao, A., Wu, S., Yan, W., Yuan, J., Liu, C., DeBuc, D.C., Wang, J., 2015. Measurement variability of the bulbar conjunctival microvasculature in healthy subjects using functional slit lamp biomicroscopy (FSLB). Microvasc. Res. 101, 15–19.